JOURNAL OF CATALYSIS **131,** 335–349 (1991)

Preparation of Platinum on Activated Carbon

H. E. VAN DAM[1] AND H. VAN BEKKUM

Organic Chemistry Department, Delft University of Technology, Julianalaan 136,
2628 BL Delft, The Netherlands

Received November 25, 1988; revised April 17, 1991

In a study of the preparation of Pt/C catalysts, a set of modified activated carbon carriers has been prepared by nitric acid or air oxidation, or thermal decarboxylation. The carbons obtained by these methods had largely identical pore structures, but differed considerably in surface chemistry. A series of activated carbons with different surface chemistry was impregnated with aqueous hydrochloroplatinic acid solutions. Upon impregnation, the carbon reduced a certain amount of the Pt^{IV} complex to Pt^{II}, which was strongly chemisorbed at the walls of the carrier's mesopores. Weak physisorption was also observed. The capacity of the carrier for the reductive chemisorption was governed by its surface chemistry, and thus was strongly dependent on the pretreatment of the activated carbon. Aqueous alkaline formaldehyde solutions were then applied as reductor. After a period of slow growth, during which small zero-valent platinum particles were formed, a critical crystallite size was reached. Subsequently, a fast autocatalytic growth was observed until the supply of unreduced platinum became rate limiting. During the reduction process the carrier surface chemistry was (slightly) modified. After the reduction was completed, a catalytic autoredox reaction of excess formaldehyde to methanol and formate was observed. By properly selecting the preparation conditions, platinum-on-carbon catalysts combining a high metal load (5%) and a high metal dispersion (60%) could be obtained. © 1991 Academic Press, Inc.

INTRODUCTION

In contrast to most inorganic carriers, activated carbons show an excellent stability in virtually all liquid media. They also allow a relatively facile recovery of the active phase. Carbon is therefore the carrier of choice in most heterogeneously catalyzed liquid phase processes in fine chemistry. Activated carbon-supported catalysts are also applied in gas phase reactions.

Platinum-on-carbon is used as catalyst for hydrogenation and, to a lesser extent, for oxidation reactions. A large number of patents and papers deal with the preparation of platinized carbon. However, most of this work is empirical in character, and little has been reported about the actual chemistry of the catalyst preparation process.

Such knowledge would greatly facilitate the design and preparation of Pt/C catalysts with desired properties. Therefore, we have investigated the catalyst preparation process in detail, including: (i) the chemical modification and characterisation of activated carbon, (ii) the impregnation of these carriers with platinum compounds, and (iii) the reduction of these impregnates to metallic Pt/C catalysts.

In the present work Norit ROX 0.8 was used as starting material. This commercially available extruded activated carbon was chosen for its purity, mechanical strength, and corresponding ease of handling. The carbon was modified by different nitric acid oxidations, air oxidation, thermal decarboxylation, or hydrogen reduction. The resulting carriers were characterized by nitrogen porosimetry, acid/base titrations, and XPS.

In the preparation of supported metal catalysts, the dispersion and distribution of the active phase are largely determined by the

---

[1] Present address: Norit Research & Development, P.O. Box 105, 3800 AC Amersfoort, The Netherlands.

0021-9517/91 $3.00

impregnation step. In the case of platinized carbon, the precursor most often used is hexachloroplatinic acid (H_2PtCl_6). This compound usually yields a better metal dispersion than, for example, platinum ammine complexes (*1*). The latter precursors result in high dispersions only when the carrier is specially pretreated to increase its ion exchange capacity (*2*). From aqueous solutions, hexachloroplatinic acid is adsorbed very strongly onto activated carbons (up to approximately 10 wt% of platinum, depending on the activated carbon). The adsorption is less strong when solutions of the platinic acid in organic solvents are used (*3*).

The chemistry of the impregnation process is still not well understood. Early XPS work (*4*) indicated that, after impregnation of activated carbon with $H_2Pt^{IV}Cl_6$ and subsequent drying in air, the platinum was present as Pt^0 and Pt^{II}. This is surprising since highly dispersed platinum metal is very sensitive to air oxidation (*5*). The effects of the carrier surface chemistry on the impregnation process are unknown.

It was decided to reinvestigate the impregnation process in detail, including the effects of some additives and the effects of variations in the surface chemistry of the carrier. Hexachloroplatinic acid was selected as the metal precursor.

The reduction of the impregnated carrier is a delicate step. However, even for such a common system as platinum-on-carbon, little is known of the actual chemistry of the reduction process. Pt/C catalysts are thus produced using "cookbook" methods based on empirical experience. Using these procedures the catalysts obtained are often far from optimal. Also, it is not possible to predict the effects of changes in the process variables.

This part of the present study was aimed at (i) gaining insight into the chemistry of the reduction process, and (ii) using this insight to obtain catalysts with different properties. One of these (intrinsic) properties is the carrier surface chemistry, which can exert an important effect on the selectivity of Pt/C oxidation catalysts (*6*).

A reduction method often used in the preparation of Pt/C catalysts is treatment with hydrogen gas at elevated temperatures (e.g., 400°C) (*7*). At these temperatures, the surface groups of the carrier are not stable. So, this procedure is not suited when the effects of the carbon surface chemistry on the properties of the catalyst are to be studied.

Alternatively, the reduction can be performed using a hydrogen donor (e.g., formaldehyde) in alkaline aqueous solutions (*8*). The effects of this reduction method on the surface chemistry of the carrier are unknown. However, the reactions can be performed at ambient temperatures, at which the carrier surface chemistry is at least thermally stable. We have therefore selected this liquid phase reduction method for our studies.

The use of hydrogen donor molecules in alkaline solutions also provided the possibility to study the relevant reactions. During the hydroxyl ion-consuming reduction processes, the pH was kept constant using a pH-stat. Plotting the alkali consumption versus time enabled a detailed study of the stoichiometry and the kinetics of the reduction reactions to be made. The products formed from the hydrogen donor were analyzed using ^{13}C NMR.

EXPERIMENTAL

Materials and Methods

Starting material. Norit ROX 0.8 activated carbon (Norit NV, Amersfoort, The Netherlands); peat-based, gas-activated extrudates (d = 0.8 mm, l = 3–5 mm); macropores 0.2–5 μm (from mercury porosimetry) were used. Total pore volume was 1.0 ml/g. Inorganic impurities *before* washing procedure included (see below): Fe 0.02%, Ca 0.02%, total ash content 3% (mostly SiO_2).

Carrier modification

Nitric acid oxidations. Carriers N5, N10, N20, and N30 were prepared by oxidation of ROX 0.8 with different amounts of nitric acid. ROX 0.8 (50 g) and water (230.8, 211.5, 173.1, and 134.6 g, respectively) were stirred and heated to 100°C. Nitric acid (65% by weight) (19.2, 38.5, 76.9, and 115.4 g, respectively) was added over 30 min, and the reaction was continued for 60 min (100–103°C, with stirring). The mixtures were cooled, poured into water, and washed (see below). Small amounts of fines were removed by flotation.

Air oxidation. Carrier A was prepared from ROX 0.8 by air oxidation for 24 h at 350°C in a rotating kiln (courtesy Norit NV).

Decarboxylation. Carrier D was prepared from ROX 0.8 by heating for 1 h at 320°C in flowing helium using a vertical tube oven.

Hydrogen treatment. Carrier H was prepared in a similar way applying hydrogen gas (3 h, 320°C) followed by passification in helium (1 h, 320°C).

Washing procedure. Prior to any use, carbon ROX as well as all modified carbons (50 g) were slowly percolated with: (i) water (5 liter); (ii) sodium hydroxide solution (0.5 *M*, 5 liter, final eluate colorless); (iii) water (5 liter); (iv) hydrochloric acid (0.5 *M*, 5 liter, final eluate salt free); and (v) water (10 liter, final pH 6), and dried overnight at ambient conditions.

Nitrogen porosimetry. Mesopore distribution and BET surface area were determined by nitrogen adsorption at −196°C using a Carlo Erba Sorptomatic 1800 apparatus.

Titration curves. Samples of the material (200 mg) were mixed with a potassium chloride solution (5 ml, 0.1 *M*). Concentrated potassium hydroxide or hydrochloric acid solutions were added. After equilibration (5 days) the pH values of the solutions were determined. Corrections were made for the capacity of the solution at extreme pH values.

XPS. X-ray photoelectron spectroscopy was performed on a Leybold Heraeus XPS/AES apparatus using Mg$K\alpha$ radiation and Shirley background correction (courtesy DSM Central Laboratory).

Impregnation

H_2PtCl_6 adsorption isotherms. Aqueous hexachloroplatinic acid (Johnson Matthey) solutions (5 ml) were added to samples of the carriers (200 mg). After 5 days of slow agitation at 20°C, equilibrium was reached. The solutions were decanted and analyzed spectrophotometrically (*9*) for their platinum content.

Acetone extractions. The impregnated carbons (200 mg) were extracted with p.a. acetone (5 ml) at 20°C for 5 days.

XPS. X-ray photoelectron spectra were recorded using a Leybold Heraeus LHS-10 XPS/AES apparatus with a HP 1000 E data system. The instrument was calibrated externally. The C 1*s* signal of the carbon was found at E_B = 284.3 eV, which coincides with the literature value (*10*). Sample charging was therefore concluded to be absent.

The impregnated activated carbon extrudates were broken to obtain fresh surfaces, stacked vertically in a sample holder, and dried *in vacuo* in the XPS apparatus. Both before and during irradiation (Mg$K\alpha$) mass spectra were recorded of the remaining gas molecules in the vacuum system, revealing m/e 35 + 37 (Cl) and 44 (e.g., CO_2). Although a slight increase in pressure was observed upon starting the excitation, differences between the Pt 4*f* spectra of samples exposed for very short and long times were insignificant. The Pt signal intensity was about 15-fold lower than expected on a simple weight basis. A similar effect has been reported for rhodium on carbon, and was attributed to the porous nature of the carrier (*11*).

Impregnates. To the carbon (100 g) and water (1000 g) a calculated amount of concentrated hexachloroplatinic acid (Johnson Matthey) solution was added in 60 equal portions at 0.5 min intervals. Between the additions the mixture was agitated to ensure an equal loading of all carrier particles. The mixture was kept for 4 days at room temperature in the dark, and the excess solution was removed by filtration. The impregnates thus obtained contained ~50% water. The (acidic) mother liquor was titrated with potassium hydroxide; the results are included in the figures as the HO^- consumptions at t = 0.

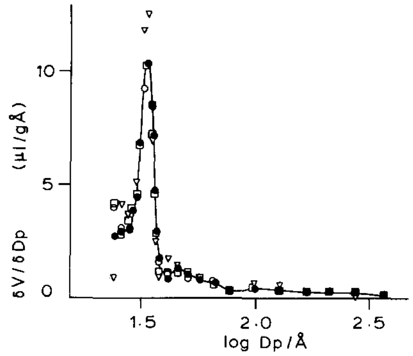

FIG. 1. Pore structures of activated carbons. (□) N30 (S_{BET} 930 m^2/g); (▽) A (1100); (●) ROX (910); (○) D (990).

Hydrothermal treatment. The moist impregnates were heated to 95°C in closed containers.

Reductions. The reductions were performed in a 50-ml screw cap vessel, equipped with a pH electrode, a reference electrode, a nitrogen gas inlet tube, a gas purge outlet, and a burette tip. The homemade reference electrode was of the double junction type, enabling stable measurements to be made in the strongly reducing reaction media. The pH was controlled automatically using a Metrohm 632 pH meter, a 614 impulsomat, and a 655 dosimat containing 2.00 *M* potassium hydroxide. The vessel was agitated continuously.

In the reduction vessel, the reductor solution (10.0 ml, 0.3–10 *M*) was added to the wet impregnate (4 g, equivalent to 2.00 g final Pt/C catalyst). The system was flushed with nitrogen gas (1 min), and the reduction was started by raising the pH to the desired value. From then on, the pH was kept constant by the pH control system. After the reduction, the catalyst was thoroughly eluted with water (to pH 7), dried (20°C, 50 mTorr, 24 h), and submitted to dispersion measurements.

The alkali consumption vs time of the separate components (e.g., the carbon) and any combination thereof (as given in Figs. 1 and 2) was obtained analogously. All displayed OH^- consumptions include the amounts necessary to initiate the desired pH value.

Dispersion measurements. These were performed using a modified Quantasorb apparatus (Quantachrome Corp.). The samples were reduced in flowing hydrogen gas (20°C, 16 h). Then, the Pt metal dispersion was determined through the adsorption of carbon monoxide pulsed into the hydrogen stream. A blank experiment showed the absence of CO adsorption onto the carrier.

^{13}C NMR. Nuclear magnetic resonance analysis of liquid samples was performed using a Nicolet NT 200 WB apparatus. The relaxation conditions chosen ensured a (semi)quantitative analysis of all reductor derived compounds.

RESULTS AND DISCUSSION

Carrier Modification

Mechanical strength. The modification methods applied did not affect the mechanical integrity of the carbon extrudate particles.

Pore structure. Figure 1 provides data on the BET equivalent surfaces and mesopore structures of some selected carriers (the other carriers gave similar results). Air oxidation caused a small increase in BET surface and mesopore volume (−20%). The other modification methods had no significant effect on the pore structure at all.

XPS. X-ray photoelectron spectra of ROX and N30 are represented in Fig. 2. Both carriers can be seen to consist only of

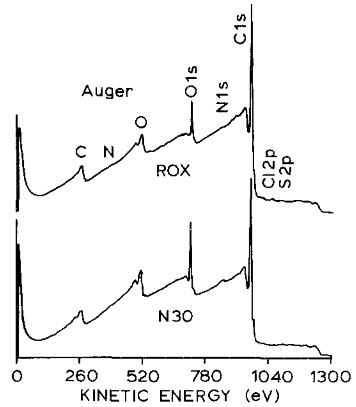

FIG. 2. XPS spectra of activated carbons ROX and N30.

carbon and oxygen (and hydrogen). Hence, nitric acid oxidation did not result in the introduction of significant amounts of nitrogen.

Titration curves. Figure 3 shows that all carriers have both acidic and basic properties. The oxidations resulted in an increased surface acidity. High-temperature treatment in helium and hydrogen (samples D and H, respectively) gave almost identical surface acidity losses. No steps, associated with discrete pK_a values, are observed in the titration curves. Since no step is found at pH$_i$ (isoelectric point), it would be possible that there is some overlap between the pK_a ranges of the acidic and basic groups, leading to zwitterionic structures at pH values around pH$_i$.

Impregnation

Types of adsorption. Figure 4 shows hexachloroplatinic acid adsorption isotherms on different carbon carriers. Part of the platinum compound (5–10 wt% platinum load, dependent on the carrier) is adsorbed very strongly. The isotherms also show a weak "equilibrium" adsorption, which is virtually independent of the surface chemistry of the carrier. This weak adsorption is likely to be a physisorption process. (Physisorption is expected to occur since hexachloroplatinic acid is soluble in both water and nonpolar solvents. It may thus act as a surfactant, reducing the surface tension between the aqueous solution and the carbon basal plane surface.) The strong adsorption section of the isotherms is now discussed further.

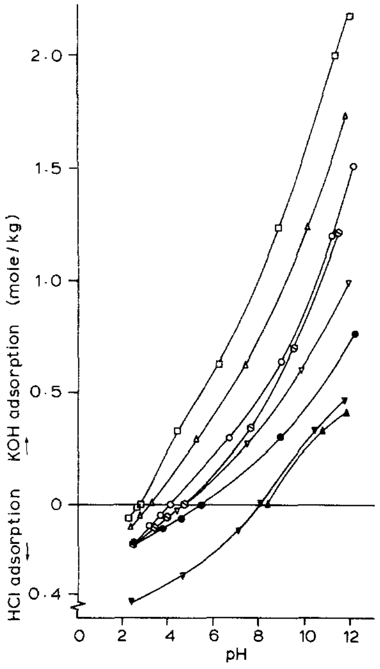

FIG. 3. Acid and base adsorption capacities of carbons as function of pH. (☐) N30; (△) N20; (○) N10; (▽) N5; (⊘) A; (●) ROX; (▼) D; (▲) H.

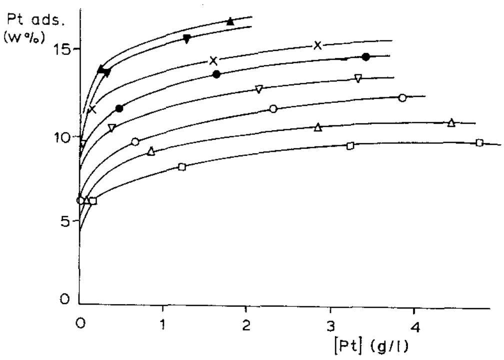

FIG. 4. Hexachloroplatinic acid equilibrium adsorption onto activated carbons with different surface chemistry (water, 25°C). carbon: (☐) N30; (△) N20; (○) N10; (▽) N5; (●) A; (×) ROX; (▼) D; (▲) H.

XPS analyses. The state of the strongly adsorbed platinum was investigated by XPS analysis. A typical Pt 4*f* spectrum is presented in Fig. 5. The spectra were not dependent on the duration of the exposure. Thus reduction caused by the radiation (*12*) may be excluded. Experimental bonding energies may be compared with the following literature values (*10*) (Pt $4f_{7/2}$: Pt^0 71.0–71.3 eV; $K_2Pt^{II}Cl_4$ 72.8–73.4 eV; $K_2Pt^{IV}Cl_6$ 74.1–74.3 eV). Deconvolution of the experimental spectrum (Fig. 5) resulted in two doublets, with Pt $4f_{7/2}$ at 72.2 eV (83%) and 74.2 eV (17%), respectively. The former, larger, doublet is to be attributed to a Pt^{II} complex with a bonding energy slightly smaller than that of $K_2Pt^{II}Cl_4$. Hence reduction of hexachloroplatinic acid does indeed (*4*) occur upon its impregnation into acti-

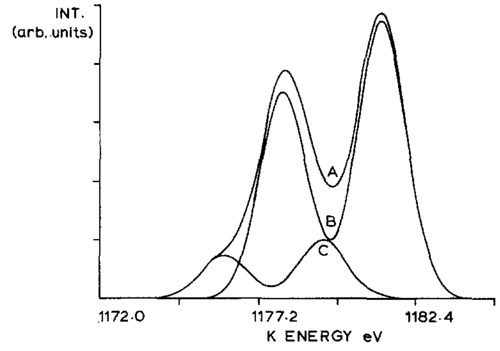

FIG. 5. XPS spectra of hexachloroplatinic acid adsorbed on carbon ROX (5% Pt). (A) Experimental spectrum. After deconvolution: (B) E_B (Pt $4f_{7/2}$) 72.2 eV; (C) E_B 74.2 eV.

vated carbon. It may be noted that polyacetylene is known to reduce Pt^{IV} in H_2PtCl_6 to Pt^{II} (*13*).

The low-intensity doublet with Pt $4f_{7/2}$ at 74.2 eV corresponds to a Pt^{IV} complex, probably $PtCl_6^{2-}$. Its intensity is increased by drying of the sample in air at 120°C. The presence of this small amount of platinum in the parent oxidation state is believed to be caused by reoxidation during the sample preparation (artifact), although its true presence cannot be excluded.

To obtain more insight into the mode of adsorption of the platinum^{II} complex on the carbon, the effects of carrier modifications and additives were studied.

Effects of carrier surface chemistry. Since all carriers have practically identical BET surfaces and pore distributions (Fig. 1), differences in adsorption behavior on differently pretreated carriers must arise from the surface chemistry of the carbons. Figure 4 shows that the strong adsorption is decreased by oxidative carrier pretreatments. This is easily explained by a decreased reductive capacity of the oxidized carriers.

Effects of additives. Figure 6 shows the effects of some ionic additives on the adsorption process. The presence of hydrochloric acid decreases the strong adsorption, which would, at first sight, point to an electrostatic adsorption mechanism: protonation of basic carrier sites, with $Pt^{II}Cl_4^{2-}$ counterions. However, while potassium chloride (no carrier protonation) shows the same effect as hydrochloric acid, methanesulfonic acid (a strong acid with a very weakly coordinating anion) has no effect at all. Thus the electrostatic mechanism given can be excluded. Since chloride ions counteract the strong adsorption of the platinum^{II} species, this process includes the loss of one or more chloride ligands. Indeed, it has been reported (*14*) that upon heating hydrochloroplatinic acid impregnated carbon at 200°C in nitrogen three HCl molecules were evolved.

Addition of ytterbium^{III} nitrate also decreased the amount of strongly bound platinum.

Effects of acetone. Figure 7 shows the results of adsorption and desorption experiments in which acetone/water (90/10) was used as solvent. Acetone itself is strongly adsorbed onto the carrier. It thus competes with the strong adsorption of H_2PtCl_6, and practically excludes the weak adsorption of the latter. A carrier impregnated with aqueous hexachloroplatinic acid can be partly depleted from its platinum load by extraction with acetone.

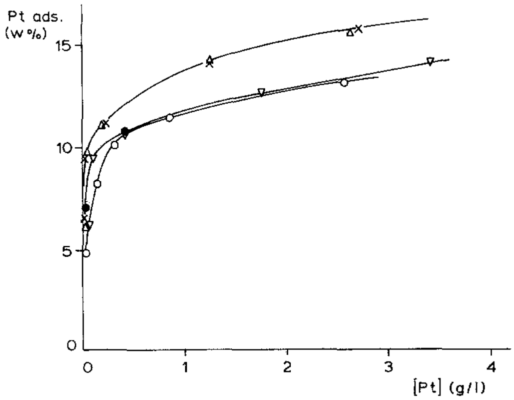

FIG. 6. Hexachloroplatinic acid equilibrium adsorption onto activated carbon ROX: effects of additives (water, 25°C). Additive (0.1 *M*): (×) none; (▽) HCl; (●) KCl; (△) methanesulfonic acid; (○) $Yb(NO_3)_3$.

SCHEME 1. Pt/C preparation processes.

Process	HO⁻ Consumption	
	HO^-/Pt	meq[a]
Impregnation		
$H_2Pt(IV)Cl_6 + \geqslant C{-}H + H_2O \longrightarrow$ $Pt(II)Cl_4^- + 2Cl^- + \geqslant C{-}O^- + 5H^+$	5	2.57[b]
$Pt(II)Cl_4^- + S \longrightarrow PtCl_3S^- + Cl^-$	—	—
Reduction		
$PtCl_3S^- + H_2C(OH)_2 + 3HO^- \xrightarrow{Pt}$ $Pt(0) + 3Cl^- + S + HCOO^- + 3H_2O$	3	1.54
Overall		
$H_2Pt(IV)Cl_6 + \geqslant C{-}H + H_2C(OH)_2 + 8HO^- \xrightarrow{Pt}$ $Pt(0) + 6Cl^- + \geqslant C{-}O^- + HCOO^- + 7H_2O$	8	4.10[c]
Hydrogen transfer		
$2H_2C(OH)_2 + HO^- \xrightarrow{Pt} HCOO^- + H_3COH + 2H_2O$		

[a] Based on 0.513 mmol platinum.
[b] See Fig. 1.
[c] See Fig. 2.

Model. A model describing the chemistry of the impregnation process is presented in Scheme 1. The carbon reduces the Pt^{IV} to Pt^{II}, which is then coordinatively bound by the carrier. A reducing site on the carrier surface is denoted as $\geqslant C{-}H$ and $\geqslant C{-}OH$ is its (acidic) oxidation product. The formation of acidic groups during the oxidation of the carrier by Pt^{IV} is deduced from titration experiments (see below). *S* denotes a ligand site for Pt^{II}. The nature of these sites, and the complexes derived therefrom, will now be discussed.

Ligand site S. Principally, two types of ligand for Pt^{II} are present on the carrier, namely C=C structures in the carbon basal planes, and oxygen-containing functional groups on the basal plane edges.

π-complex structures. The platinum complexes can be repelled from the carrier by organic solvents (*3*) such as acetone. This would point to adsorption on the carbon basal planes (acetone itself is not a strong ligand for Pt^{II} (*15*)). Activated carbon can be regarded as a very bulky C=C ligand. Complexation with bulky ligands is stereochemically unfavorable. However, platinum complexes can be described in terms of bonding and back-bonding, i.e. electron donation from a filled π orbital of the ligand to an empty orbital of the metal, and back-donation from the metal to an empty π* orbital of the ligand (*16*). Activated carbon has a high-valence band edge (~HOMO) and a low-conduction band edge (~LUMO) (*17*), and therefore a very favorable electronic structure for coordination of Pt^{II}.

For two reasons, π-complex formation would take place preferentially at the perimeter of the carbon basal planes. First, these sites are sterically favored. By analogy with *cis*-alkene Pt complexes, the platinum ion may bend away from the "substituents" of the C=C ligand (*16*) (this is especially so since the basal planes in activated carbon are thought to be somewhat puckered). Second, theoretical calculations (*18*) indicate

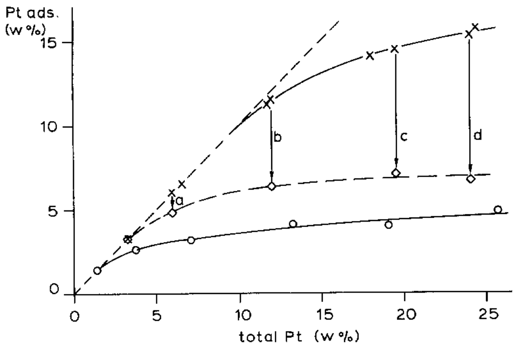

FIG. 7. Hexachloroplatinic acid equilibrium adsorption onto activated carbon ROX, and extraction with acetone (25°C). Adsorption: (×) from aqueous solution; (○) from acetone solution. (a–d) acetone extractions; (◇) adsorbed after extraction.

that the sites with the smallest electron localization energy are found at the edges. The armchair edge features pairs of reactive carbon atoms. At the zigzag edge, very reactive sites are alternating with particularly unreactive C-atoms (this picture may, however, be altered by the presence of conjugated oxygen surface groups).

Recently, a similar π-complex formation has been suggested for the adsorption of copper^{I} chloride complexes onto activated carbon (*19*).

*Oxygen-containing complex structures.*Addition of ytterbium nitrate (Fig. 6) decreases the strong adsorption. Hard ions such as Yb^{III} do not form π-complexes. Hence the effect of Yb^{III} is more easily explained when the strong adsorption of platinum is considered to take place on weak donor ligands containing oxygen atoms (denoted O-ligands). Although not all are very stable, several complexes of Pt^{II} with O-ligands are known, e.g., acetylacetonates and carboxylates (*20*). Many such ligand structures are present at the edges of the carbon basal planes. More will be formed in the oxidation of the carbon during the $H_2Pt^{IV}Cl_6$ adsorption process. Thus formation of Pt^{II} O-ligand complexes seems possible.

Location of platinum complexes in the carrier. Both types of coordination (i.e., π-complexation or "oxygen" complexation) would take place at the edges of the basal plane structures. Although the present work does not allow the exclusive identification of the exact structures of the complexes, it can be concluded that the Pt^{II} ions formed during the impregnation are bound at the basal plane edges, i.e., at the walls of the mesopores.

Basic Reduction Processes

Platinum absent. Figures 8 and 9 (curves a, b) show the titration curves at pH 11 for (i) the parent carbon carrier (Norit ROX 0.8), and (ii) the carrier plus the formaldehyde solution used as reductor. The acidic groups on the carbon surface naturally consume HO^-. This process is not very fast, and is (at least partly) controlled by the diffusion of hydrated potassium ions to those acidic groups that are located within the carbon micropores. (Hydroxyl ions and pro-

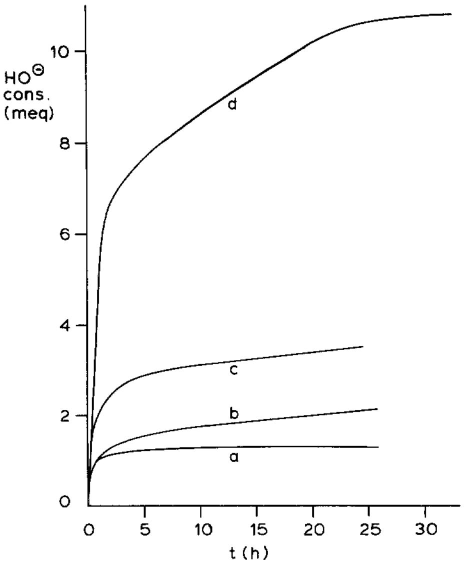

FIG. 8. Alkali consumption vs time of basic catalyst preparation processes. (a) ROX (1.90 g); (b) ROX + methylene glycol (10 ml 1 *M*); (c) H_2PtCl_6/ROX (0.513 mmole Pt); (d) H_2PtCl_6/ROX + methylene glycol.

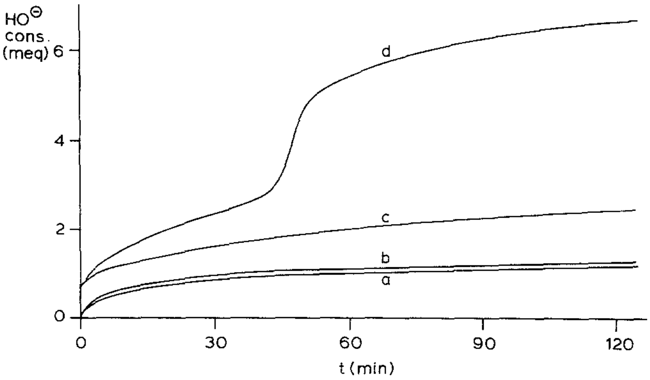

FIG. 9. Alkali consumption vs time of basic catalyst preparation processes (as Fig. 8, initial 2 h in detail). (a–d) See legend Fig. 8.

tons migrate very fast by the interconversion of covalent and hydrogen bonds.) Formaldehyde in diluted aqueous media is principally present as methylene glycol ($H_2C(OH)_2$) (*21*), denoted as MG (1 *M* solution: ~90% MG, ~10% dimer). At pH 11, the reductor (MG $pK_a \approx 13$ (*21*)) did not consume a significant amount of hydroxyl ions; also the present conditions do not induce a noticeable homogeneous Cannizzaro reaction. The combination ROX + MG showed a slightly enhanced hydroxyl ion consumption, indicating a slow (cross) Cannizzaro type reaction involving the carbon (either as reactant or as catalyst).

H_2PtCl_6/ROX. The titration of ROX impregnated with hexachloroplatinic acid resulted in a HO^- consumption, which was ultimately 2.5 meq above the ROX titration value (Fig. 8, curve c). It has been shown above that during the impregnation $H_2Pt^{IV}Cl_6$ is reduced to a platinum^{II} complex by the carbon. From the present data (Scheme 1) it is concluded that, during this oxidative impregnation of the carrier, acidic groups are formed.

H_2PtCl_6/ROX + MG. As demonstrated in Fig. 9 (curve d), the actual catalyst preparation process proceeds autocatalytically. Initially, the curve follows the sum of the H_2PtCl_6/ROX titration and the consumption of hydroxyl ions through the interaction of the reductor and the carrier: [H_2PtCl_6/ROX + MG] = [H_2PtCl_6/ROX] + [ROX + MG] − [ROX]. Then, the actual platinum reduction becomes noticeable and proceeds at an increasing rate. This acceleration may be explained as follows. Initially, very small Pt^0 crystallites will be formed (see below). On these nucleation centers the reductor (MG) will adsorb dissociatively. This results in the formation of chemisorbed hydrogen atoms and (desorbed) formate ions (and possibly some carbonate, see below). The platinum^{II} complexes are reversibly adsorbed by the carbon and therefore mobile (through liquid or surface diffusion). When they reach the hydrogen-covered nucleation centers, the complexes will be reduced to Pt^0. This leads to an increasing metal surface, and thus to an accelerated Pt^{II} reduction rate. As a result the platinum crystallites catalyze their own growth. (Similar effects occur in electrodeless plating and in photographic development.)

The reduction of platinum complexes to Pt^0 by hydrogen-covered Pt crystallites is a known process (*22*).

Initial Pt^0 nuclei. The formation of initial Pt^0 nuclei is a key factor in any reduction mechanism leading to platinum crystallites. From the steepness of the fast autocatalytic growth (Fig. 9), it follows that (i) fast growth occurs after the crystallites reach a critical size, and, since disperse catalysts can be obtained, (ii) a large number of crystallites reach this critical size at the same time.

The occurrence of a critical size logically follows from the absence of subsurface hydrogen adsorption sites (*26*) in crystallites smaller than 6 atoms. Assuming that at least two subsurface sites are necessary to accommodate, in a reactive mode, the 2 hydrogen atoms supplied by the dehydrogenation of the reductor, a critical crystallite size of 10 atoms is deduced. Smaller crystallites will adsorb hydrogen only in a much less reactive form, comparable to the (very strongly adsorbed) hydrogen on edge atoms of larger crystallites.

Many crystallites reach their critical size at approximately the same time. The nucleation of the crystallites is thus also likely to take place at the same time, logically when the reduction process is started. This implies that the nuclei are either already present in the impregnate, or that a fraction of the platinum^{II} is in a reactive form, yielding nuclei as soon as the reduction is started.

The number of nuclei will normally be small compared to the total number of Pt atoms in the system (e.g., when the metal dispersion is 0.4 the crystallites contain approximately 1000 atoms), and well below the detection limits of, for example, XPS. Therefore only indirect data on the number of initial nuclei can be obtained.

Pt^0-catalyzed hydrogen transfer. Figure 8 shows that after the reduction of the platinum complexes is completed, a further reaction takes place. The experiment was repeated and samples of the liquid phase were analyzed by ^{13}C NMR (Fig. 10). The consecutive reaction is identified as a (Pt^0-catalyzed) hydrogen transfer from one molecule of (hydrated) formaldehyde to another, yielding formate ions (HO^- constant) and methanol. This autoredox process is included in Scheme 1. It strongly resembles the earlier reported hydrogen transfer from glucose to fructose (*23*).

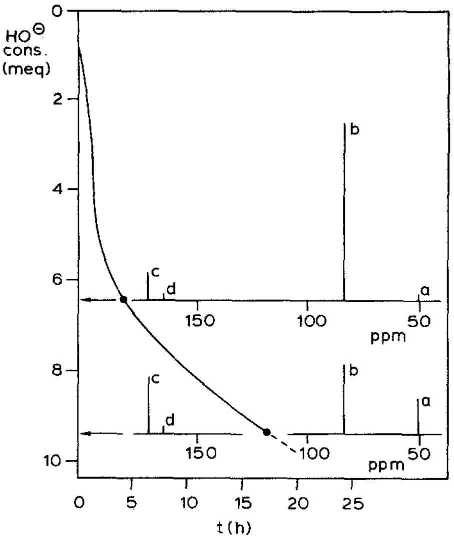

FIG. 10. Alkali consumption vs time and ^{13}C NMR spectra of liquid phase samples: autoredox reaction of formaldehyde. H_2PtCl_6/ROX (0.513 mmole Pt)/ROX (1.90 g) + methylene glycol (10 ml 1 *M*). (a) Methanol; (b) methylene glycol; (c) formate; (d) (bi)carbonate.

Figure 10 also shows that in the actual Pt^{II} reduction process methylene glycol is converted into formate ions. Only a small fraction of these ions is further oxidized to carbonate.

Other reductors. The catalyst preparation was also performed using other reducing species, i.e., methanol, potassium formate, and (dissolved) hydrogen (see Fig. 11). As expected, the autocatalytic effect was observed in all cases, whereas the hydrogen transfer reaction was specific for methylene glycol reductions.

When hydrogen gas was used as reducing species, the reduction rate was probably controlled by the supply of hydrogen. The low solubility of this gas in water is expected to result in a diffusion-controlled reaction at the outer part of the carbon extrudate. This would lead to a scale-type catalyst with a low metal dispersion (see below).

*Carbon surface chemistry.*An interesting point is the effect of the catalyst preparation on the carrier surface chemistry. It may be

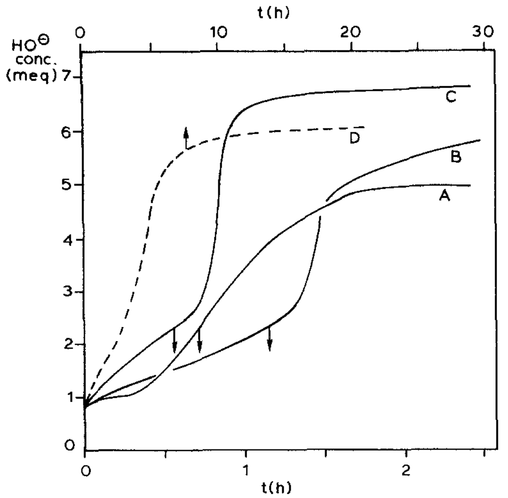

FIG. 11. Alkali consumption vs time of catalyst preparation processes: different reductors. H_2PtCl_6/ROX (0.513 mmole Pt)/ROX (1.90 g) + reductor (10 ml 1 *M*). Reductor (pH): (A) hydrogen (10); (B) methylene glycol (10); (C) formate (11); (D) methanol (10) (upper time scale).

expected that a platinum crystallite is able to modify catalytically the carbon surface groups in its surroundings. After reduction, the platinum is located (mainly) in the mesopores (*24*). The walls of these pores partly consist of carbon basal plane edges, i.e., carbon surface groups.

The titration data in Fig. 11 revealed a small excess hydroxyl ion consumption during the catalyst preparation. Hence ionizable acidic groups are formed. Also, during the preparation of (0.5%) platinum on ROX, the oxygen content of the carrier (as determined by thermolysis–GC) was found to decrease from 3.3 to 2.3% wt%). The number of surface groups is thus decreased.

At the pH values used in the catalyst preparation, most of the acidic groups are ionized. These groups are expected to be stable toward reduction. Carbonyl groups, however, may be hydrogenated catalytically to hydroxyl groups (which will then be partly ionized in the alkaline medium), or completely removed. More decisive conclusions would require an analytical tool that is able to focus on the carbon surface chemistry surrounding the platinum crystallites.

Metal Dispersion

Key factors. The dispersion (*D*) of Pt/C catalysts prepared by the liquid phase reduction method will be governed by: (i) the number of crystallites reaching the critical size at the same time, and therefore the number of initial nuclei, (ii) the rate of transportation of Pt(II) complexes to the growing crystallites, and (iii) the rate of reduction of the complexes on the metal surface.

Rate-limiting step. When the Pt^{II} reduction on the crystallite surface is the rate-limiting step (i.e., the Pt^{II} diffusion is relatively fast), the growth rate of a crystallite will be proportional to its surface area. Hence large crystallites will grow faster than small crystallites. This finally results in a small number of very large crystallites, i.e., a low metal dispersion.

When the Pt^{II} diffusion to the crystallite surface is rate limiting (i.e., the Pt^{II} reduction on the Pt^0 surface is relatively fast), all crystallites will grow at an equal rate. This will result in a high metal dispersion.

The autocatalytic effect (Fig. 9) occurs in all preparation reactions. In the beginning of the reduction process the actual reduction is rate limiting. Then, after the critical crystallite size is reached, the reaction rate on the growing Pt^0 surface increases rapidly, and the amount of unreduced Pt^{II} complexes decreases. Thus at a certain point the diffusion of Pt^{II} complexes becomes the limiting factor, and the overall rate decreases again. An optimal dispersion will thus be obtained when (i) a high number of initial nuclei is present, (ii) the Pt(II) reduction on the crystallite surface is fast, and (iii) the Pt(II) complex diffusion is slow.

Table 1 shows the effects of variations in the reduction conditions and the carbon carrier on the time lapse before the fast growth phase begins, and on the catalyst metal dispersion. This dispersion is expressed as the ratio of carbon monoxide adsorbed (as determined by CO adsorption in

TABLE 1

Effects of Reduction Conditions on Metal Dispersion and Time Lapse before Fast Growth Phase

Variable[a]	Value	Dispersion (CO/Pt)	Time lapse (min)
Reductor concentration (*M*)	0.3	0.38	180
	1.0	0.40	90
	3.0	0.29	55
	10.0	0.20	35
pH	10	0.40	90
	11	0.40	50
	12	0.25	15
Carrier	D	0.40	60
	ROX	0.40	90
	A	0.36	50
	N5	0.27	95
	N10	0.26	80
	N20	0.21	80
	N30	0.10	70
Reductor	$HCOO^-$	0.35	50
	$H_2C(OH)_2$[b]	0.40	90
	H_3COH	0.13	250
	H_2	0.14	—[c]

[a] 5% Pt loading in all cases. Reference system: carbon ROX, 1 *M* methylene glycol, pH 10.
[b] pH 11.
[c] See text.

hydrogen gas at room temperature (*25*)) and platinum present. The results can be discussed on the basis of the key factors mentioned above.

Reductor concentration. The use of methylene glycol concentrations higher than 1 *M* resulted in lower metal dispersions. A concentration of 1 *M* seems sufficient to ensure an optimal reduction rate, i.e., to keep the crystallite surface covered with hydrogen. A too high reductor concentration may have two negative effects. The reductor is adsorbed by the carrier, competing with the Pt^{II} adsorption (cf. the effect of acetone on the adsorption (*6*)). The reductor may also compete with the Pt^{II} complexes in the adsorption on the crystallites, thus decreasing the Pt^{II} reduction rate (cf. Langmuir–Hinshelwood kinetics). Hence a higher MG concentration leads to an enhanced Pt^{II} mobility and perhaps a decreased Pt^{II} reduction rate, both leading to a lower dispersion.

pH. Increasing the pH leads to a higher carrier surface negative charge. The Pt^{II} surface complexes are also negatively charged. For this reason, increasing the pH will lead to an increased electrostatic repulsion between the carrier and the Pt^{II} species. This results in a higher mobility of the complexes and therefore a lower metal dispersion.

Carrier surface chemistry. The carrier surface negative charge is also dependent on the carbon pretreatment (Table 2). Again the expected decrease in the dispersion with increased surface negative charge is observed. However, the surface chemistry may also affect the number of initial nuclei. The stronger oxidized carriers could produce a smaller number of (zero-valent) plati-

TABLE 2

Characteristic Data on Carriers Used

Carrier	Modification method	Oxygen content (wt%)	pH$_i$	Surface negative charge (pH 10) (mole/HG)
ROX	—	3.3	5.5	0.43
N5	Nitric acid oxidation (5–30% acid)	5.6	4.7	0.62
N10		8.0	4.1	0.87
N20		9.3	3.3	1.23
N30		12.4	2.8	1.60
A	Air oxidation 320°C	8.8	4.7	0.82
D	Helium 320°C	2.7	8.1	0.27
R	Hydrogen 320°C	Not determined	8.4	—

num nuclei, which would also lead to the observed effect.

Reductor. Methylene glycol and formate (Fig. 11) show comparable reactivities and yield similar dispersions. Methanol is much more difficult to dehydrogenate and therefore less reactive. Also it is less polar and therefore better adsorbed by the carrier. Methanol as reductor thus yields poor metal dispersions. When using hydrogen, the reduction also proceeded slowly and largely as a zero-order process, probably because of the low solubility of hydrogen in the liquid phase. It is likely that only crystallites in the outer shell of the catalyst extrudate particle benefit from the reduction. The resulting dispersion is indeed very low.

Hydrothermal treatment. It was thought that the formation of nuclei would be enhanced by an increase in temperature. Therefore, part of the impregnate was stored at higher temperatures prior to the reduction. The effect of this "hydrothermal treatment" is demonstrated in Table 3. A treatment temperature of 65°C had little effect, but keeping the wet impregnates at 95°C for several days resulted in a significantly increased dispersion. This increase was, however, only obtained when the reduction of the impregnates was performed immediately after the temperature treatment. Storing the treated impregnates for 3 weeks prior to reduction resulted in the "normal" dispersion equaling 0.36–0.40 (this may be caused by annealing of nuclei formed at higher temperatures).

Platinum loading. The effect of the platinum loading on the platinum dispersion (Fig. 12) is dependent on the reduction method used. At favorable reduction conditions, a high dispersion that decreases with increasing metal load is obtained. At unfavorable reduction conditions the dispersion is generally much smaller but load-independent. In the latter case, the crystallites are probably limited in size by the carbon (meso)pore system (*24*).

CONCLUSIONS

The chemical modification methods applied to Norit ROX 0.8 resulted in a set of carbon carriers with virtually identical pore structures, but with widely varying (pH-dependent) surface charges. The oxidized carriers have a moderate to strongly increased surface acidity.

Upon impregnation into activated carbon, hexachloroplatinic acid is (partly) converted into a Pt^{II} complex. This complex is strongly

TABLE 3

Effect of Hydrothermal Treatment of Impregnate on Dispersion of Catalyst

Reductor	Temperature (°C)	Duration (h)	Dispersion (CO/Pt)
$HCOO^-$	—	—	0.35
	—	—	0.34
	65	16	0.43
	65	43	0.40
	95	3.5	0.49
	95	22	0.54
	95	65	0.60
	95	164	0.54
$H_2C(OH)_2$	—	—	0.40
	—	—	0.38
	95	20	0.52
	95	70	0.58
	95	93	0.57

Note. 5% Pt on carbon ROX, 1M methylene glycol, pH 10.

bound at the walls of the mesopores, as a π-complex and/or through ligands containing oxygen. Addition of hydrochloric acid decreases the interaction between the carrier and the noble metal compound, and should be avoided in the catalyst preparation process.

The liquid phase reduction of activated carbon impregnated with hexachloroplatinic acid proceeds from nuclei present at or directly after the beginning of the reduction process. After a critical crystallite size has been reached, rapid autocatalytic growth occurs until the diffusion of the (largely carbon surface bound) platinum complexes to the growing crystallites becomes rate limiting.

The number of nuclei, the intrinsic reduction rate, and the platinum complex diffusion rate all affect the final dispersion of the noble metal phase. Well-dispersed catalysts are obtained when (i) the impregnated carbon is given a heat treatment (to improve the number of nuclei), (ii) a low concentration of reductor is used (to avoid displacement of platinum complexes from the carrier), (iii) a carrier is applied with a small number of acidic groups, (iv) the pH is not too high (to prevent electrostatic repulsion between the carrier surface and the platinum complexes), and (v) the applied hydrogen donor is reactive enough to keep the platinum crystallites occupied with (subsurface) hydrogen.

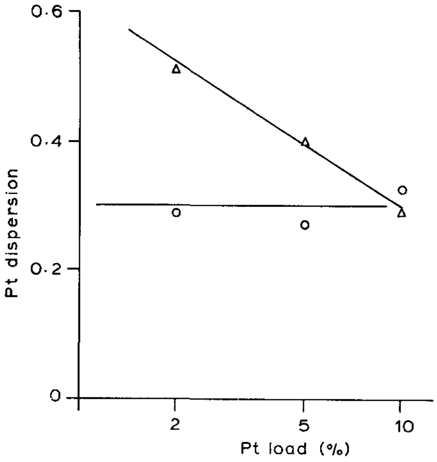

FIG. 12. Platinum dispersion vs loading of Pt/C catalysts, prepared by different methods. (△) 1 *M* methylene glycol, pH 10; (○) 5 *M* methylene glycol, pH 12.

ACKNOWLEDGMENTS

The authors are indebted to J. Teunisse and N. van Westen for nitrogen porosimetry and dispersion measurements, to J. A. Peters for NMR analyses, to W. Brouwer (DSM Central Laboratory, Geleen) for XPS analyses, to J. J. F. Scholten for his kind mediation, and to J. Reedijk for valuable discussions. The financial support of the Netherlands Organisation for Scientific Research (NWO) is gratefully acknowledged.

REFERENCES

1. Palmer, M. B., and Vannice, M. A., *J. Chem. Tech. Biotechnol.* **30,** 205 (1980).
2. Richard, D., Gallezot, P., *in* "Preparation of Catalysts" (B. Delmon, P. Grange, P. A. Jacobs, and G. Poncelet, Eds.), p. 71. Elsevier, Amsterdam 1987.
3. Hanika, J., Machek, V., Nemec, V., Ruzicka, V., and Kunz, J., *J. Catal.* **77,** 248 (1982); and references therein.
4. Czaran, E., Finster, J., and Schnabel, K.-H., *Z. Anorg. Allg. Chem.* **443,** 175 (1978).
5. Stokes, H. T., Makowka, C. D., Wang, P.-K., Rudaz, S. L., and Slichter, C.P., *J. Mol. Catal.* **20,** 321 (1983).
6. Okunowski, J. K., Van Dam, H. E., Van Bekkum, H., *Recl. Trav. Chim. Pays-Bas* **109,** 103 (1990).
7. E.g. Rodriguez-Reinoso, F., Rodriguez-Ramos, I., Moreno-Castilla, C., Guerrero-Ruiz, A., and Lopez-Gonzalez, J. D., *J. Catal.* **99,** 171 (1986).
8. E.g., Zelinski, N. D., and Turowa-Polyak, M. B., *Chem. Ber.* **58,** 1298 (1925).
9. Ayres, G. H., and Meyer, A. S., *Anal. Chem.* **23,** 299 (1951).
10. "Handbook of X-ray Photoelectron Spectroscopy." Perkin–Elmer Corp., 1979; Briggs, D., Seah, M. P.,"Practical Surface Analysis." Wiley, New York, 1983.
11. Brinen, J. S., and Schmitt, J. L., *J. Catal.* **45,** 274 (1976).
12. Katrib, A., *J. Electron Spectrosc. Relat. Phenom.* **18,** 275 (1980).
13. Cao, Y., Guo, K., and Oian, R., *Huaxue Xuebao* **43,** 425 (1985).
14. Uhlir, M., Hanika, J., Sporka,K., and Ruzicka, V., *Collect. Czech. Chem. Commun.* **42,** 2791 (1977).
15. Davis, J. A., and Hartley, F. R., *Chem. Rev.* **81,** 79 (1981).
16. Hartley, F. R., *Chem. Rev.* **69,** 799 (1969); **73,** 163 (1973).
17. McMichael, B. D., Kmetko, E. A., and Mrozowski, S., *J. Opt. Soc. Am.* **44,** 26 (1954).
18. Stein, S. E., and Brown, R. L., *Carbon* **23,** 105 (1985).
19. Hirai, H., Wada, K., and Komiyama, M., *Bull. Chem. Soc. Jpn.* **60,** 441 (1987).
20. Hartley, F. R., "The Chemistry of Platinum and Palladium" Applied Science, London, 1973.
21. Walker, J. F., "Formaldehyde," 3rd ed. Krieger, Huntington, NY, 1975.
22. Menezo, J. C., Denanot, M. F., Peyrovi, S., and Barbier, J., *Appl. Catal.* **15,** 353 (1985).
23. De Wit, G., Thesis, Delft University of Technology, 1979.
24. Van Dam, H. E., Duijverman, P., Kieboom, A. P. G., and Van Bekkum, H., *Appl. Catal.* **33,** 373 (1987).
25. Anderson, J. R., "Structure of Metallic Catalysts," p. 311. Academic Press, London, 1975; Scholten, J. J. F., Pijpers, A. P., and Hustings, A. M. L., *Catal. Rev.-Sci. Eng.* **27,** 151 (1985).
26. Eberhardt, W., Greuter, F., and Plummer, E. W., *Phys. Rev. Lett.* **46,** 1085 (1981); Lagos, M., *Surf. Sci.* **122,** L601 (1982).